The Inducible CXCR3 Ligands Control Plasmacytoid Dendritic Cell Responsiveness to the Constitutive Chemokine Stromal Cell–derived Factor 1 (SDF-1)/CXCL12

Béatrice Vanbervliet,[1] Nathalie Bendriss-Vermare,[1] Catherine Massacrier,[1] Bernhard Homey,[2] Odette de Bouteiller,[1] Francine Brière,[1] Giorgio Trinchieri,[1] and Christophe Caux[1]

[1]*Laboratory for Immunological Research, Schering-Plough, 69571 Dardilly, France*
[2]*Department of Dermatology, Heinrich-Heine University, D-40225 Düsseldorf, Germany*

Abstract

The recruitment of selected dendritic cell (DC) subtypes conditions the class of the immune response. Here we show that the migration of human plasmacytoid DCs (pDCs), the blood natural interferon α–producing cells, is induced upon the collective action of inducible and constitutive chemokines. Despite expression of very high levels of CXCR3, pDCs do not respond efficiently to CXCR3 ligands. However, they migrate in response to the constitutive chemokine stromal cell–derived factor 1 (SDF-1)/CXCL12 and CXCR3 ligands synergize with SDF-1/CXCL12 to induce pDC migration. This synergy reflects a sensitizing effect of CXCR3 ligands, which, independently of a gradient and chemoattraction, decrease by 20–50-fold the threshold of sensitivity to SDF-1/CXCL12. Thus, the ability of the constitutive chemokine SDF-1/CXCL12 to induce pDC recruitment might be controlled by CXCR3 ligands released during inflammation such as in virus infection. SDF-1/CXCL12 and the CXCR3 ligands Mig/CXCL9 and ITAC/CXCL1 display adjacent expression both in secondary lymphoid organs and in inflamed epithelium from virus-induced pathologic lesions. Because pDCs express both the lymph node homing molecule L-selectin and the cutaneous homing molecule cutaneous lymphocyte antigen, the cooperation between inducible CXCR3 ligands and constitutive SDF-1/CXCL12 may regulate recruitment of pDCs either in lymph nodes or at peripheral sites of inflammation.

Key words: dendritic cells • chemokines • migration • regulation • virus

Introduction

Plasmacytoid DCs (pDCs) were first characterized as plasmacytoid monocytes/T cells accumulating around the high endothelial venule (HEV) of inflamed lymph nodes (for review see reference 1), and later identified as a $CD11c^-$ DC subset from blood and tonsils characterized by a plasmacytoid morphology and a unique surface phenotype ($CD4^+$ IL-$3R^{2+}$ $CD45RA^+$ HLA-DR^+; 1–3). Recently, pDCs have been demonstrated in human (4, 5) and mouse (6) to be the natural IFN-α–producing cells, in response to viruses (for review see reference 1). After exposure to viruses, pDCs induce a potent in vitro priming and Th-1 polarization of naive T cells, through IFN-α and possibly IL-12 (7, 8). Although still unclear, the expression of lymphoid markers and the lack of myeloid antigens suggest a lymphoid origin of pDCs (2, 3, 9). Compared with myeloid DCs, pDCs are activated by different signals in accordance with different Toll-like receptor expression (10).

Under homeostasis, pDCs have not been reported in peripheral nonimmune tissues, suggesting a different migratory capacity compared with myeloid DCs. Immature myeloid DCs respond to many inflammatory chemokines and are recruited at site of inflammation (11, 12). In particular, MIP-3α/CCL20 recruits Langerhans cells most likely in combination with the inflammatory CCR2 ligands (13). After antigen uptake at site of infection, the induced expression of CCR7 allows maturing myeloid

Address correspondence to Christophe Caux, Laboratory for Immunological Research, Schering-Plough, 27 chemin des Peupliers, BP 11, 69571 Dardilly, France. Phone: 33-4-72-17-27-00; Fax: 33-4-78-35-47-50; email: christophe.caux@spcorp.com

Abbreviations used in this paper: HEV, high endothelial venule; pDC, plasmacytoid DC; SDF-1, stromal cell–derived factor 1.

 J. Exp. Med. © The Rockefeller University Press • 0022-1007/2003/09/823/8 $8.00
Volume 198, Number 5, September 1, 2003 823–830
http://www.jem.org/cgi/doi/10.1084/jem.20020437

DCs to emigrate to the draining lymph node and elicit immune responses (11, 12, 14).

Unlike myeloid DCs, pDCs, which express L-selectin, have been proposed to enter the lymph node from the blood (5). However, only recently has information regarding the migratory capacity of pDCs been reported (15–17).

Here we report observations arguing for a cooperation between constitutive and inflammatory chemokines both in pDC entry in the lymph node from blood, and in their recruitment at peripheral inflammatory sites.

Materials and Methods

Hematopoietic Factors, Reagents, and Cell Lines. 2.10^6 U/mg hGM-CSF (Schering-Plough Research Institute), 2.10^7 U/mg rhTNF-α (Genzyme), 4.10^5 U/mg rhSCF (R&D Systems), and 2.10^7 U/mg rhIL-4 (Schering-Plough Research Institute) were used at 100 ng/ml, 2.5 ng/ml, 25 ng/ml, and 50 U/ml, respectively. Recombinant human chemokines were from R&D Systems (13).

Enrichment for CD11c⁻ pDCs and CD11c⁺ Myeloid DCs from Peripheral Blood and In Vitro Generation of DCs from Cord Blood CD34⁺ Hematopoietic Progenitor Cells and Monocytes. Human peripheral blood was obtained anonymously from the Establissement Francais du sang after the donor gave informed consent according to the Declaration of Helsinki specifically indicating the possible research use of the sample if it was not suitable for transfusion use. Discarded human surgical material (tonsils and cord blood) was obtained anonymously according to the institutional regulations in compliance with French law. Circulating blood CD11c⁻ pDCs and myeloid CD11c⁺ DCs were prepared from peripheral blood as previously described (2, 13). Lineage⁺ cells were removed from mononuclear cells using antibodies and magnetic beads (anti–mouse Ig-coated Dynabeads; Dynal). The enriched population contained 10–30% CD11c⁻ pDCs and 15–25% CD11c⁺ myeloid DCs, identified on the expression of HLA-DR (tricolor; Becton Dickinson), CD11c (PE; Becton Dickinson), and lack of lineage markers (FITC). For some experiments, cells were further purified by FACS® sorting based on the above triple staining.

Positively selected cord blood CD34⁺ cells were cultured for 6 d in the presence of SCF, GM-CSF, TNF-α, and 5% AB⁺ human serum as previously described (13).

Monocyte-derived DCs were produced by culturing monocytes purified by immunomagnetic depletion for 6–7 d in the presence of GM-CSF and IL-4 (14). T cell subsets were isolated from peripheral blood by immunomagnetic depletion.

Analysis of Chemokine Receptor Expression by FACS®. For blood CD11c⁻ pDCs, receptor expression was determined by triple staining on enriched blood DC populations and gating on Lin⁻, CD11c⁻ (FITC), and HLA-DR⁺ (tricolor) using PE-coupled antibodies. Similarly, for CD11c⁺ myeloid DCs, receptor expression was determined by triple staining gated on Lin⁻, CD45RA⁻ (FITC), and HLA-DR⁺ (tricolor). After this protocol the CD11c⁻ pDCs were 95–98% CD45RA⁺ and IL-3Rα⁺, and the CD11c⁺ myeloid DCs were 95–98% CD11c⁺, IL-3Rα⁻.

CD34-derived DCs or monocyte-derived DCs were processed for double staining using FITC-conjugated CD1a or CD14 and PE-conjugated mAbs.

PE anti-hCCR3 (61628.111) was from R&D Systems. PE anti-hCXCR4 (51505.111), hCCR5 (2D7), hCCR6 (11A9), and hCXCR3 (1C6) were from BD Biosciences. Biotinylated anti-hCCR1 (53504.111) and hCCR2 (48607.211) from R&D Systems, were revealed by streptavidin-PE (DakoCytomation). Anti-hCCR7 (2H4) was a mouse IgM (BD Biosciences) revealed by biotin-coupled goat anti–mouse IgM (Caltag). PE anti-CD83 (Immunotech) and PE anti–IL-3Rα, FITC anti-CLA, and PE anti-CD62L (BD Biosciences) were also used.

Chemotaxis Assay in Transwells. Migration assays were performed using transwell (6.5 mm diameter; COSTAR) with 5×10^5 cells/well as previously described (13). Enriched blood DC populations were first preincubated for 2 h at 37°C and then placed for 2 h in 5-μm pore size inserts. The migration was revealed by triple staining gated on CD11c⁻/HLA-DR⁺/lineage⁻ and CD11c⁺/ HLA-DR⁺/ lineage⁻. Monocytes, monocyte-derived DCs, and day 6 CD34⁺ hematopoietic progenitor cell–derived DC precursors were incubated for 1–2 h in 5-μm pore size inserts and migration was revealed by CD1a/CD14 double staining. T cells were incubated for 1 h in 3-μm pore size inserts and migration was revealed by CD3/CD45RA double staining.

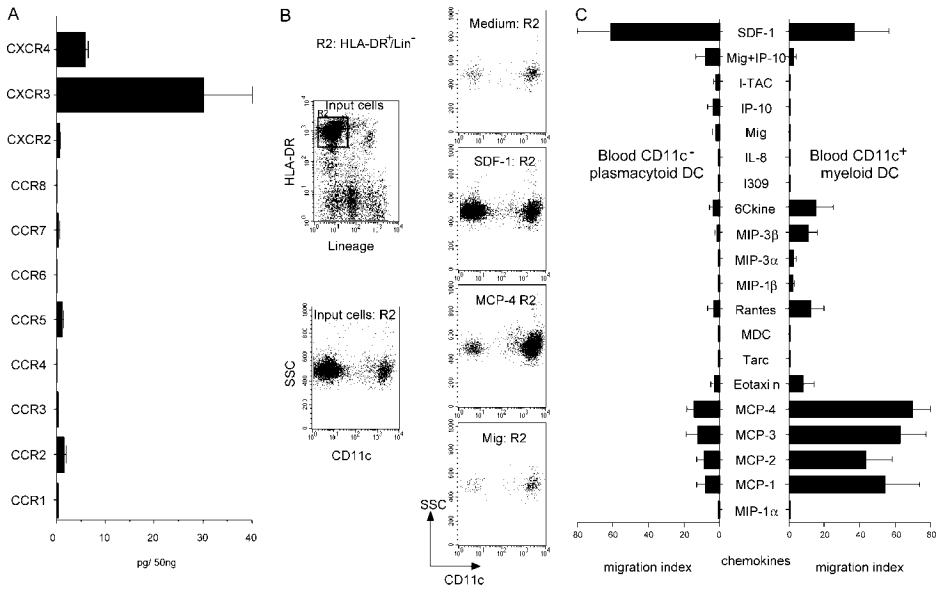

Figure 1. pDCs do not respond to most inflammatory chemokines. (A) Quantitative PCR for chemokine receptors on FACS®-sorted pDCs. Results expressed as pg/50 ng total RNA were normalized using 18S RNA (mean of $n = 3$). (B) Enriched circulating blood DC subsets were rested for 2 h at 37°C and then studied in transwell (5-μm pore size) migration assay. Examples of CD11c FACS® profiles of gated HLA-DR⁺ lineage marker⁻ migrating cells (representative of ≥ 10). (C) Responses of blood CD11c⁻ pDCs and CD11c⁺ myeloid DCs to various chemokines. Each chemokine was tested over a wide range of concentrations (1–1,000 ng/ml) and only the optimal response is shown ($n \geq 5$).

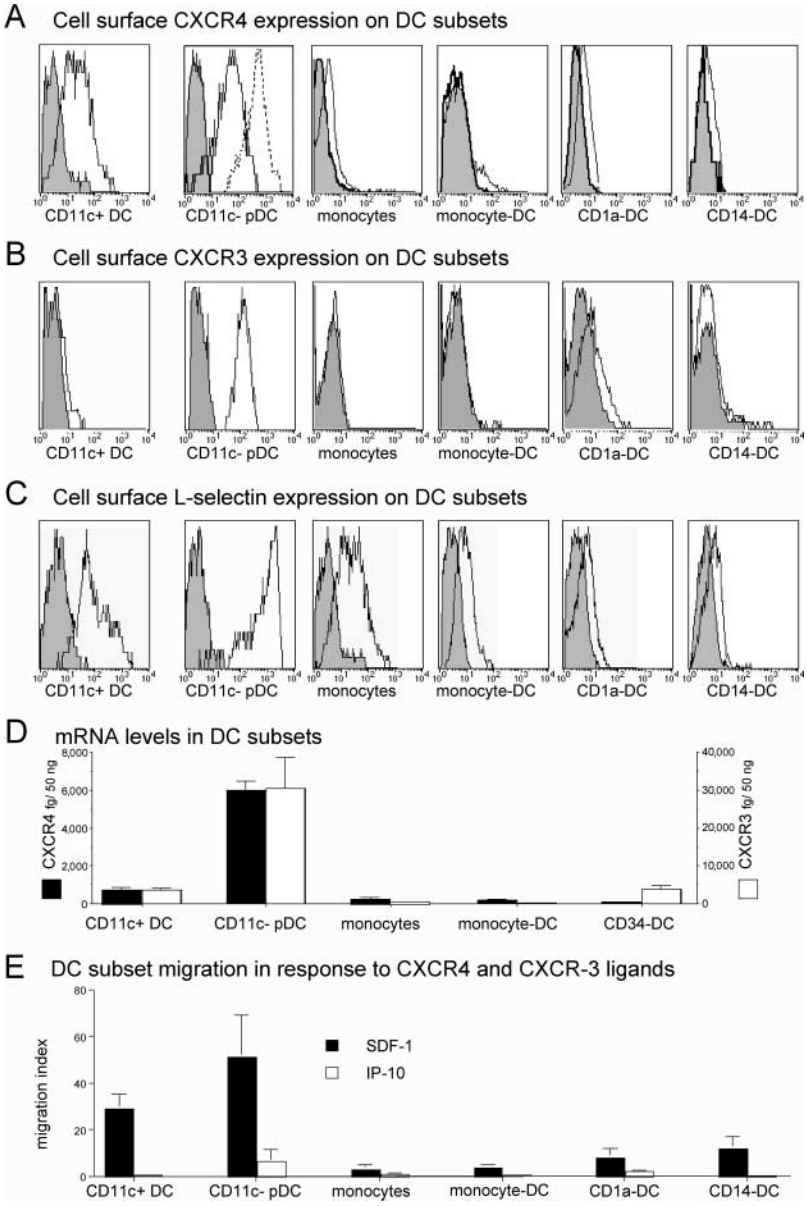

Figure 2. Potent activity of the constitutive chemokine SDF-1/CXCL12 and high CXCR4, CXCR3, and L-selectin expression on pDCs. CXCR4 (A), CXCR3 (B), and L-selectin (C) cell surface expression on DC population (representative of ≥3). For pDC CXCR4, expression was also analyzed after 2 h of preincubation at 37°C (A, dashed line). mRNA expression of CXCR4 and CXCR3 was also determined by quantitative PCR (D) on the same populations (results expressed as pg/50 ng total RNA were normalized using 18S RNA, mean of $n = 3$). Finally, optimal response to CXCR4 and CXCR3 ligands is shown for each DC population (E, mean of $n \geq 5$).

Results were expressed either as migration index (ratio chemokine/medium) ± standard deviations, or as number of migrating cells (mean of duplicate experimental points). <10% variations were observed in these experiments.

Quantitative Real-Time PCR (TaqMan) Analyses of Chemokine Receptor mRNA Expression. Cells were prepared as described above. Total RNA was extracted, reverse transcribed, and cDNA amplified in the presence of TaqMan universal master mix (PerkinElmer) and gene-specific FAM-labeled TaqMan probe and gene-specific forward and reverse primers (PerkinElmer) as previously described (13). As an internal positive control, 18S RNA-specific JOE- or VIC-labeled TaqMan probe and primers were added to each reaction. Gene-specific PCR products were measured with an ABI PRISMÆ 7700 Sequence Detection System (PerkinElmer) during 40 cycles. Target gene expression was normalized between different samples based on the 18S RNA values.

Immunohistochemistry. Human tissue specimens were obtained after the donor gave informed consent according to the Declaration of Helsinki specifically indicating the possible research use of the sample and according to the institutional review board from the hospital (B. Homey, Research Laboratory for Dermatoimmunology and Oncology Moorenstr, Düsseldorf, Germany). Frozen 6-μm tissue sections (human tonsils and skin) were fixed in acetone (13) and nonspecific activities blocked with avidin D, biotin solutions (Blocking kit; Vector Laboratories), and 0.3% hydrogen peroxide (Sigma-Aldrich). After incubation with blocking serum for 30 min, sections were immunostained with two of the following antibodies: rabbit polyclonal anti–CD62P (BD Biosciences) and mouse mAb anti–hMig/CXCL9 (mIgG1, 49106.11; R&D Systems), anti-hSDF1/CXCL12 (mIgG2a, K15C; reference 18), anti–hE-cadherin (IgG1, HECD-1; Takara), and anti-hCD105 (IgG1, 266; BD Biosciences) for 1 h at room temperature in a humid atmosphere. Rabbit Ig was detected by biotinylated goat anti–rabbit Ig (BA 1000; Vector Laboratories) and extravidin-peroxidase (Sigma-Aldrich), mouse IgG1 was revealed by sheep anti–mouse IgG1 (Binding Site) and APAAP (DakoCytomation), and

mouse IgG2a was revealed by sheep anti–mouse IgG2a coupled to peroxidase (Binding Site). The peroxidase and alkaline phosphatase activities were revealed using 3-amino-9-ethylcarbazole substrate (SK-4200; Vector Laboratories) and alkaline phosphatase substrate III (SK-5300; Vector Laboratories), respectively. Negative controls using isotype control primary antibodies were established.

Immunofluorescence for frozen 6-μm tissue sections were fixed in acetone before the immunostaining and processed as described above to block nonspecific activities. Sections were immunostained with two of the following antibodies: rabbit polyclonal anti–ITAC/CXCL11 (R&D Systems) and mouse mAb anti–CD105, and anti-hSDF1/CXCL12 followed by goat anti–rabbit IgG coupled to Alexa Fluor 488 and anti–mouse IgG coupled to Alexa Fluor 594 (Molecular Probes) for 30 min. Negative controls using isotype control primary antibodies were established.

Results and Discussion

pDCs Migrate in Response to the Constitutive Chemokine Stromal Cell–derived Factor 1 (SDF-1)/CXCL12 and Express High Levels of L-selectin. Freshly isolated human pDCs expressed cell surface CCR2 and CCR5 at comparable levels to CD11c$^+$ blood DCs (not depicted), in agreement with a recent study (15). However, unlike blood CD11c$^+$ DCs (Fig. 1) and other DC subsets (12, 13, 15), pDCs only marginally responded to CCR2 (MCPs) and CCR5 (RANTES/CCL5) ligands (Fig. 1). pDCs neither significantly expressed CCR1, CCR3, CCR4, CCR6, CCR, CXCR1, CXCR2, CXCR5 as detected by cytofluorometry (not depicted), and/or RT-PCR (Fig. 1 A), nor did they respond to their ligands (Fig. 1 C). In contrast, pDCs highly expressed CXCR4 and CXCR3 both at mRNA and surface protein levels (Figs.1 A and 2, A, B, and D). However, although pDCs migrated efficiently in response to the CXCR4 ligand SDF-1/CXCL12 with an IC50 of ~100 ng/ml (Figs. 1, B and C, 2 E, and 3 A), they only marginally respond to CXCR3 ligands (Figs. 1 C and 2 E). Compared with other DC subsets, SDF-1/CXCL12 was preferentially active on pDCs (Fig. 2 E), likely as a consequence of high CXCR4 mRNA (Fig. 2 D) and protein (Fig. 2 A), further increased at cell surface upon 2 h culture (Figs. 2 A and 4 C). SDF-1/CXCL12 displays a constitutive but restricted expression pattern in situ, with selective expression on dermal endothelial cells (18) and in lymph node HEVs (17). pDCs are primarily localized within the T

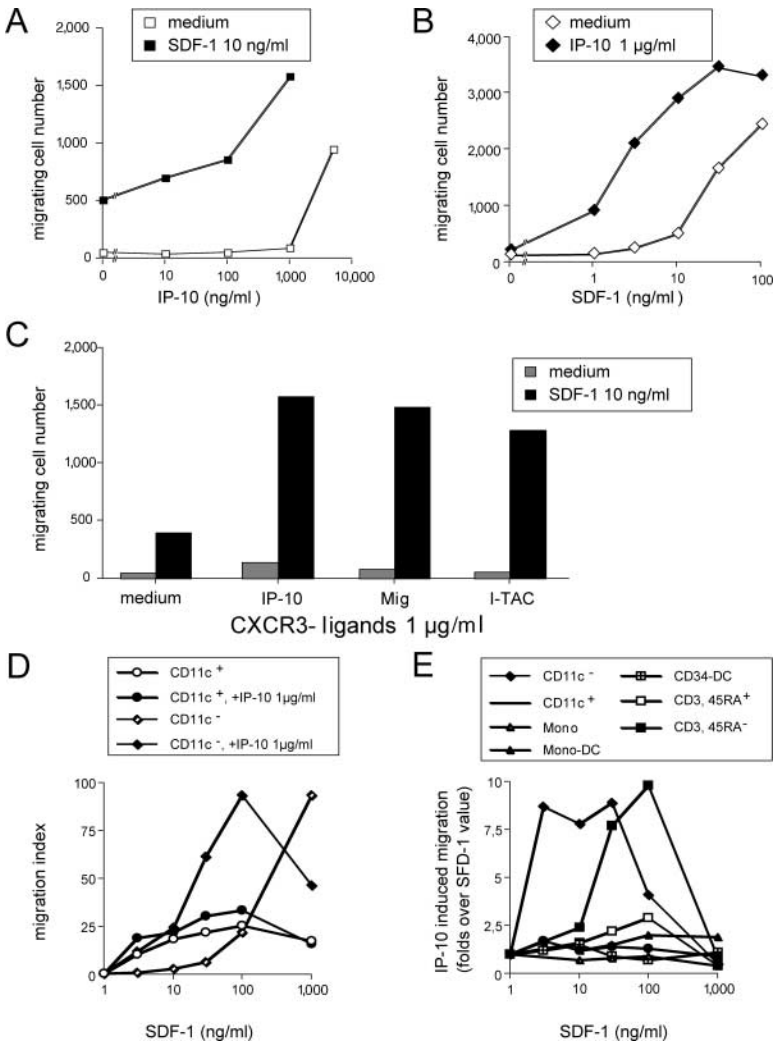

Figure 3. CXCR3 ligands selectively induce pDCs to respond to low SDF-1/CXCL12 concentration. (A) Dose response to IP-10/CXCL10 of pDCs in the presence or absence of a low dose of SDF-1/CXCL12 (10 ng/ml). (B) Dose response to SDF-1/CXCL12 of pDCs in the presence or absence of 1 μg/ml IP-10/CXCL10. (C) Response of pDCs to all CXCR3 ligands (1 μg/ml), tested individually, in the presence or absence of a low dose of SDF-1/CXCL12 (10 ng/ml). (D) Dose response to SDF-1/CXCL12 of FACS®-sorted CD11c$^-$ pDCs and CD11c$^+$ myeloid DCs in the presence or absence of 1 μg/ml IP-10/CXCL10. (E) Effects of 1 μg/ml IP-10/CXCL10 on the dose response to SDF-1/CXCL12 of various DC and T cell populations. Results are expressed as folds of IP-10–induced migration over that of SDF-1/CXCL12 alone (ratio migration index in SDF-1/CXCL12 + IP-10/CXCL10/migration index in SDF-1/CXCL12 alone). Results from $n \geq 3$.

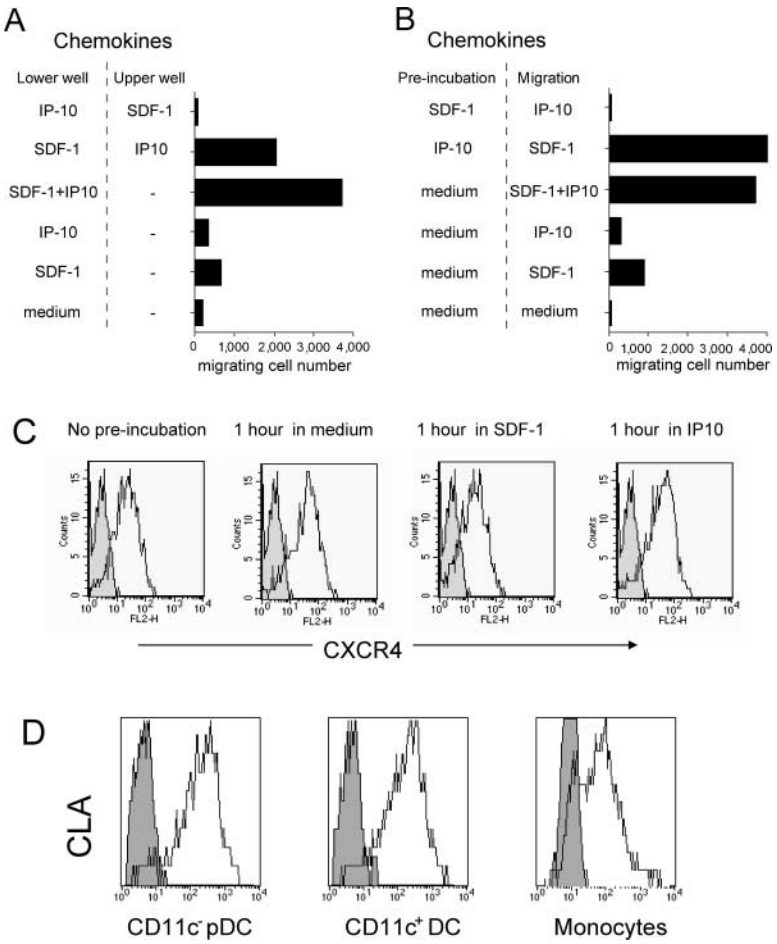

Figure 4. CXCR3 ligands prime pDCs to respond to low SDF-1/CXCL12 concentrations. (A) Experiments were performed as a typical transwell migration assay with 20 ng/ml SDF-1/CXCL12 and 1 μg/ml IP-10/CXCL10, except that the upper well can also contain a chemokine. When both the upper and lower wells contain the same chemokine, the migration was identical or lower to that in medium alone (not depicted). (B) Preincubation experiments wherein the cells were first incubated in the presence of 20 ng/ml SDF-1/CXCL12 and 1 μg/ml IP-10/CXCL10 for 1 h before performing the migration assay to both receptor ligands in transwell. When the same chemokine was used in the preincubation and in the migration assay, the migration was identical or lower to that in medium alone (not depicted). Results are from $n \geq 3$. (C) pDCs were incubated in presence of 20 ng/ml SDF-1/CXCL12, 1 μg/ml IP-10/CXCL10, or medium for 1.5 h at 37°C before performing the staining for CXCR4 (representative of $n = 3$). (D) CLA expression was performed on the different DC populations and monocytes by triple or double staining (representative of $n = 4$).

cell area of inflamed lymphoid organs, around the HEV (1). In agreement with a previous study (5), pDCs expressed much higher levels of L-selectin than other DC subsets (Fig. 2 C), at a density comparable to that of naive T cells.

The constitutive expression of SDF-1/CXCL12 and of L-selectin ligands on HEVs might be responsible for the trafficking of pDCs from the blood to the lymph nodes in homeostatic conditions. This hypothesis is supported by the observed pDC deficiency in lymph nodes from L-selectin–deficient mice (19). Thus, pDC migration could be reminiscent of that of naive T cells from the blood to the lymph nodes through L-selectin ligands and the CCR7 ligand 6Ckine/CCL21 expressed by HEV (11). However, CCR7 ligands are unlikely to be involved for resting pDC recruitment as they lack CCR7 expression. The model proposed here would imply that unlike myeloid DCs that capture pathogens in peripheral tissues and consequently migrate in lymph nodes, pDCs are constitutively recruited in lymph nodes, where they might be exposed to infectious agents.

The Inducible CXCR3 Ligands Regulate pDC Responsiveness to the Constitutive Chemokine SDF-1/CXCL12. Among chemokine receptors in pDCs, CXCR3 was expressed at the highest level (Fig. 1 A) and was absent on all other DC populations as detected by immunofluorescence at cell surface, or by quantitative RT-PCR (Fig. 2, B and D). However, only high concentrations (1–5 μg/ml) of the CXCR3 ligands IP-10/CXCL10, Mig/CXCL9, and I-TAC/CXCL11 induced significant but modest migration of pDCs (Figs. 1 C and 3, A and C). In the presence of a suboptimal dose of SDF-1/CXCL12 (10 ng/ml), IP-10/CXCL10 at a lower concentration (100–1,000 ng/ml) induced brisk migration of pDCs (Fig. 3 A). In combination with SDF-1/CXCL12, all CXCR3 ligands dramatically decreased the threshold of SDF-1/CXCL12 sensitivity by 20–50-fold (Fig. 3, B and C). These observations were confirmed on purified FACS®-sorted pDCs (Fig. 3 D) and extend a very recent study (17).

With FACS®-sorted $CD11c^+$ circulating blood "myeloid DCs," no synergistic activity was observed (Fig. 3 D). Also, neither the other DC populations tested (monocyte-derived DCs and CD34-derived DC subsets) nor naive T cells displayed synergistic response (Fig. 3 E), in agreement with the lack of CXCR3 expression on these cells. However, a synergistic activity was observed in $CD3^+$ $CD45RA^-$ memory T cells that coexpress CXCR4 and CXCR3 (Fig. 3 E).

To investigate the mechanism of the synergy, SDF-1/CXCL12 and CXCR3 ligands were opposed in upper and lower wells (Fig. 4 A). Synergy was observed when SDF-1/CXCL12 and IP-10/CXCL10 were added together in

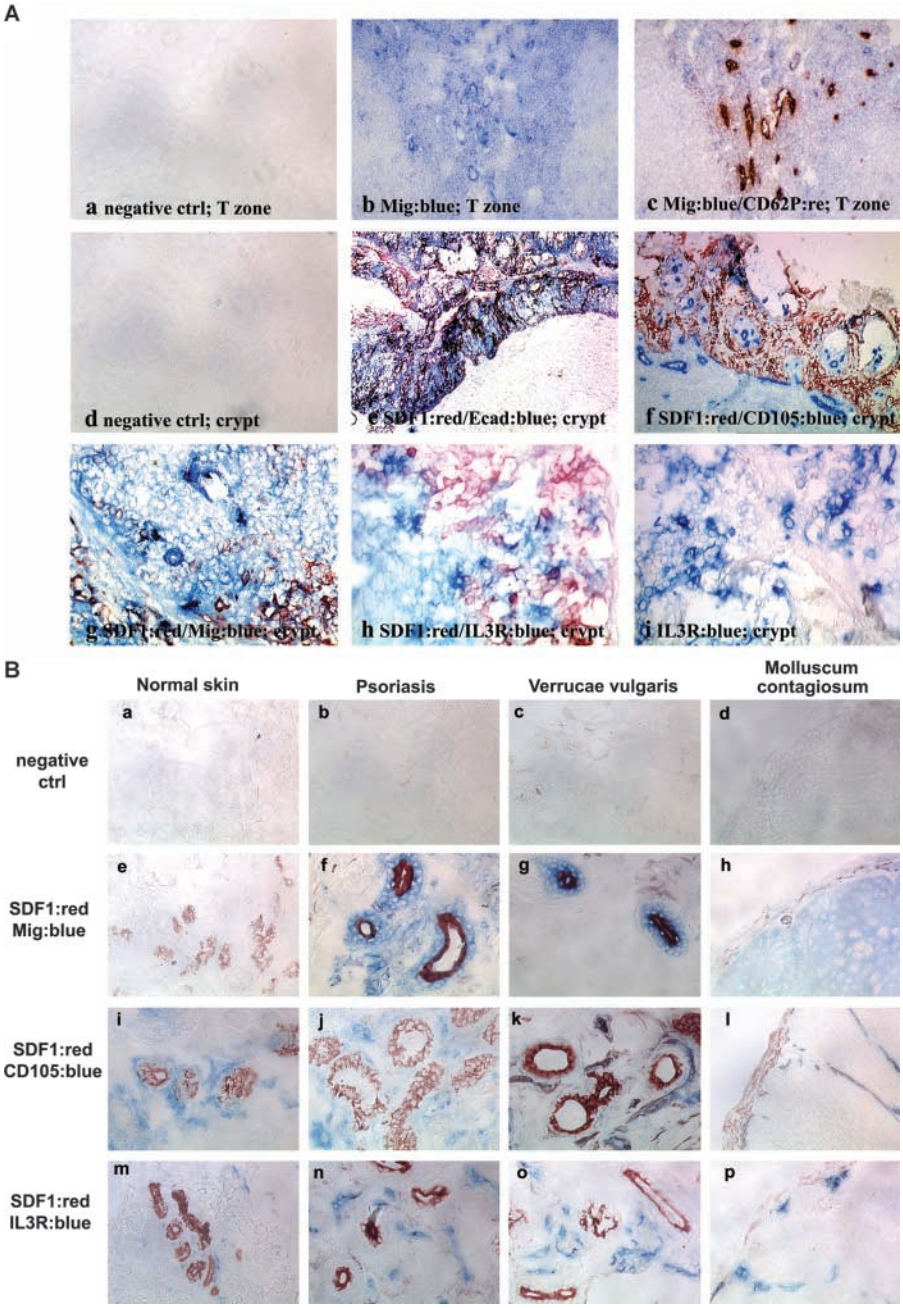

Figure 5. Mig/CXCL9 and ITAC/CXCL11 expression in blood vessels of T cell area of tonsils and of inflamed epithelium, is adjacent to that of SDF-1/CXCL12 by epithelial cells and in close contact with IL-3R–expressing pDCs. (A) Immunohistochemistry in 6-μm tonsil serial sections fixed in acetone showing detection of Mig/CXCL9 by endothelial cells in the T cell area (b and c) and in the crypt (g) contacting epithelial cells expressing SDF-1/CXCL12 (e and f) and IL-3R$^+$ pDCs (h and i) within the network of SDF-1/CXCL12$^+$ epithelial cells. Isotype match controls were performed (a, the T cell area; d, the epithelial crypt). a–c, ×200; d–f, ×100; g–i, ×400. (B) Immunohistochemistry in 6-μm serial sections fixed in acetone from normal skin, psoriatic lesion, and biopsies of *verrucae vulgaris* and *molluscum contagiosum* showing Mig/CXCL9 (e–h) expression in lesions by cells contacting CD105$^+$ blood vessels (i–l) and epithelial sites of constitutive SDF-1/CXCL12 expression (sweat gland; e–l), infiltrated by IL-3R–expressing pDCs (m–p). The specificity of the immunostainings was demonstrated using isotype match controls (a–d). ×400. (C) Immunofluorescence in 6-μm serial sections fixed in acetone showing adjacent ITAC/CXCL11 expression to that of SDF-1/CXCL12 by epithelial cells in tight contact with blood vessels in epithelial crypt of tonsils (d and g) and in sweat gland of both normal (e and h) and psoriatic (f and i) skin. The specificity of the immunostainings was demonstrated using isotype match controls (a–c). ×400. All of these observations were reproduced on more than three independent specimens.

the lower well (4.5-fold increase), as well as when IP-10/CXCL10 was in the upper well together with pDCs and SDF-1/CXCL12 in the lower well (threefold increase). In the reverse condition, no migration was observed. Similarly when pDCs were preincubated with IP-10/CXCL10, a three- to fivefold increased response to SDF-1/CXCL12 was observed, whereas SDF-1/CXCL12 did not prime them for responsiveness to IP-10/CXCL10 (Fig. 4 B). Identical results were obtained with the other CXCR3 ligands (not depicted). When similar experiments were performed with other chemokines (CCR2 or CCR5 ligands combined with CXCR3 ligands), no synergy was observed (not depicted).These results show that CXCR3 ligand activity was independent of a gradient, thus not linked to chemoattraction, and was likely due to a sensitization of the cells that allowed them to respond to lower SDF-1/CXCL12 concentrations. CXCR3 ligand activity was CXCR3 mediated as CXCR3 down-regulation was observed. The increase in SDF-1/CXCL12 responsiveness was not due to CXCR4 up-regulation as preincubation in IP-10/CXCL10 had no detectable effects on CXCR4 expression (Fig. 4 C). The CXCR3 ligands are inflammatory chemokines induced by IFN and other activators. Induction of IP-10/CXCL10 and Mig/CXCL9 primarily mediated by IFN-α/β has been shown in several mouse and primate models within hours after virus challenge (20–23).

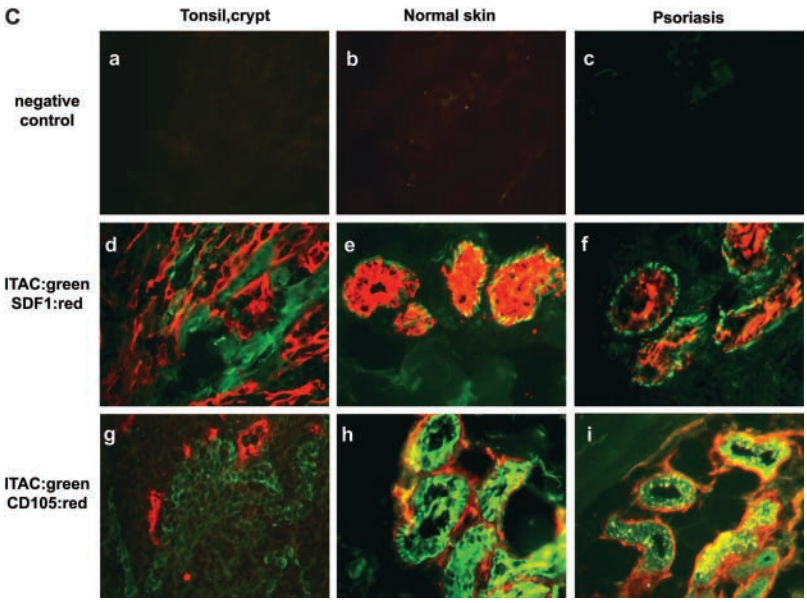

These observations, together with the recently published study on mouse pDCs (17), suggest that during viral infection or other inflammatory responses the induction of CXCR3 ligands might drive the recruitment of pDCs, and a subset of memory T cells, at sites of constitutive SDF-1/CXCL12 production. These observations represent, to our knowledge, the first descriptions that the activity of constitutive chemokines can be controlled by inflammatory chemokines.

The CXCR3 Ligands Mig/CXCL9, ITAC/CXCL11, and SDF-1/CXCL12 Display Adjacent Expression Both in Lymphoid Organs and in Inflamed Epithelial Surfaces. The distribution of SDF-1/CXCL12 and CXCR3 ligands in inflamed tissues was studied by immunohistology on tonsil, psoriatic lesions, and biopsies of *verrucae vulgaris* and *molluscum contagiosum* (Fig. 5). In the T cell area of tonsils, Mig/CXCL9 was expressed by endothelial cells in few blood vessels (Fig. 5 A, b and c). Although SDF-1/CXCL12 has been recently reported to be expressed in lymph nodes by endothelial cells (17), it was not detectable in the T cell area in tonsils (not depicted). In contrast, SDF-1/CXCL12 was strongly expressed by the network of epithelial cells in the crypt but not by $CD105^+$ endothelial cells (Fig. 5 A, e and f). Mig/CXCL9 expression was observed in the same area, possibly in blood vessels contacting the basal layer of the crypt expressing SDF-1/CXCL12 (Fig. 5 A, g). By immunofluorescent staining, ITAC/CXCL11 expression was detected on epithelial cells contacting in most instances those expressing SDF-1/CXCL12 and blood vessels (Fig. 5 C, d and g). Furthermore, pDCs detected by IL-3R expression were observed within the network of crypt epithelial cells expressing SDF-1/CXCL12 (Fig. 5 A, h and i). On normal skin and nonlesional skin (not depicted), high SDF-1/CXCL12 expression was detected by epithelial cells (E-cadherin$^+$; not depicted) of sweat glands (Fig. 5 B, e, i, and m) but not by basal keratinocytes (not depicted) as previously reported (18), whereas Mig/CXCL9 expression was not detected (Fig. 5 B, e). In contrast, in psoriatic skin, Mig/CXCL9 was highly expressed, always in close association with blood vessels and epithelial cells of sweat glands expressing SDF-1/CXCL12 (Fig. 5 B, f and j). Similarly, ITAC/CXCL11 was systemically expressed in cells in tight association with blood vessels or endothelial cells themselves, surrounding SDF-1/CXCL12 expressing epithelial sweat glands, both in normal and psoriatic skin (Fig. 5 C, e, f, h, and i). Finally, in most instances in biopsies of viral-induced skin inflammation, Mig/CXCL9 (Fig. 5 B, g, h, k, and l) and ITAC (not depicted) expression contacted epithelial structures expressing SDF-1/CXCL12 and blood vessels. Furthermore, these structures were surrounded by IL-3R–expressing cells. Although some of these IL-$3R^+$ cells might represent endothelial cells, the isolated IL-3R cells were pDCs (Fig. 5 B, n–p), as confirmed by stainings with the pDC markers BDCA4 and BDCA2 (not depicted).

From these observations, it can be hypothesized that during viral dissemination, the cooperation between CXCR3 ligands and SDF-1/CXCL12 may control the recruitment of pDCs from blood both in the draining lymph node as well as into the site of infection itself. This is consistent with the expression of the cutaneous homing molecule CLA by pDCs like other circulating DCs and monocytes (Fig. 4 D). This is in agreement with the presence of pDCs documented in the nasal mucosa (24) and in skin from patients suffering from *Lupus erythematosus* (25), in which SDF-1/CXCL12 production was previously reported (18). Finally, the first clinical manifestation of a particular leukemia representing tumorogenic pDCs (26) is the occurrence of cutaneous lesions likely due to the infiltration of leukemic pDCs (27). This represents another argument to suggest that normal pDCs might also have the capacity to reach nonlymphoid tissues.

We are grateful to C. Alexandre and M. Vatan for editorial assistance.

N. Bendriss-Vermare is a recipient of a grant from Fondation Marcel Mérieux, Lyon, France.

Submitted: 10 March 2002
Revised: 7 July 2003
Accepted: 24 July 2003

References

1. Galibert, L., C.R. Maliszewski, and S. Vandenabeele. 2001. Plasmacytoid monocytes/T cells: a dendritic cell lineage? *Semin. Immunol.* 13:283–289.
2. Grouard, G., M.C. Rissoan, L. Filgueira, I. Durand, J. Banchereau, and Y.J. Liu. 1997. The enigmatic plasmacytoid T cells develop into dendritic cells with IL-3 and CD40-ligand. *J. Exp. Med.* 185:1101–1111.
3. Res, P.C., F. Couwenberg, F.A. Vyth-Dreese, and H. Spits. 1999. Expression of pTalpha mRNA in a committed dendritic cell precursor in the human thymus. *Blood.* 94:2647–2657.
4. Siegal, F.P., N. Kadowaki, M. Shodell, P.A. Fitzgerald-Bocarsly, K. Shah, S. Ho, S. Antonenko, and Y.J. Liu. 1999. The nature of the principal type 1 interferon-producing cells in human blood. *Science.* 284:1835–1837.
5. Cella, M., D. Jarrossay, F. Facchetti, O. Alebardi, H. Nakajima, A. Lanzavecchia, and M. Colonna. 1999. Plasmacytoid monocytes migrate to inflamed lymph nodes and produce large amounts of type I interferon. *Nat. Med.* 5:919–923.
6. Asselin-Paturel, C., A. Boonstra, M. Dalod, I. Durand, N. Yessaad, C. Dezutter-Dambuyant, A. Vicari, A. O'Garra, C. Biron, F. Brière, et al. 2001. Mouse type I IFN-producing cells are immature APCs with plasmacytoid morphology. *Nat. Immunol.* 2:1098–1100.
7. Cella, M., F. Facchetti, A. Lanzavecchia, and M. Colonna. 2000. Plasmacytoid dendritic cells activated by influenza virus and CD40L drive a potent TH1 polarization. *Nat. Immunol.* 1:305–310.
8. Kadowaki, N., S. Antonenko, J.Y. Lau, and Y.J. Liu. 2000. Natural interferon α/β–producing cells link innate and adaptive immunity. *J. Exp. Med.* 192:219–226.
9. Bendriss-Vermare, N., C. Barthelemy, I. Durand, C. Bruand, C. Dezutter-Dambuyant, N. Moulian, S. Berrih-Aknin, C. Caux, G. Trinchieri, and F. Briere. 2001. Human thymus contains IFNa-producting CD11c− and myeloid CD11c+ dendritic cells as well as mature interdigitating dendritic cells. *J. Clin. Invest.* 107:835–844.
10. Kadowaki, N., S. Ho, S. Antonenko, R.W. Malefyt, R.A. Kastelein, F. Bazan, and Y.J. Liu. 2001. Subsets of human dendritic cell precursors express different Toll-like receptors and respond to different microbial antigens. *J. Exp. Med.* 194:863–869.
11. Sallusto, F., and A. Lanzavecchia. 2000. Understanding dendritic cell and T-lymphocyte traffic through the analysis of chemokine receptor expression. *Immunol. Rev.* 177:134–140.
12. Dieu-Nosjean, M.C., A. Vicari, S. Lebecque, and C. Caux. 1999. Regulation of dendritic cell trafficking: a process which involves the participation of selective chemokines. *J. Leukoc. Biol.* 66:252–262.
13. Vanbervliet, B., B. Homey, I. Durand, C. Massacrier, S. Ait-Yahia, O. De Bouteiller, A. Vicari, and C. Caux. 2002. Sequential involvement of CCR2- and CCR6-Ligands for immature dendritic cell recruitment: possible role at inflamed epithelial surfaces. *Eur. J. Immunol.* 32:231–242.
14. Dieu, M.C., B. Vanbervliet, A. Vicari, J.M. Bridon, E. Oldham, S. Aït-Yahia, F. Brière, A. Zlotnik, S. Lebecque, and C. Caux. 1998. Selective recruitment of immature and mature dendritic cells by distinct chemokines expressed in different anatomic sites. *J. Exp. Med.* 188:1–14.
15. Penna, G., S. Sozzani, and L. Adorini. 2001. Selective usage of chemokine receptors by plasmacytoid dendritic cells. *J. Immunol.* 167:1862–1866.
16. Penna, G., M. Vulcano, S. Sozzani, and L. Adorini. 2002. Differential migration behavior and chemokine production by myeloid and plasmacytoid dendritic cells. *Hum. Immunol.* 63:1164–1171.
17. Krug, A., R. Uppaluri, F. Facchetti, B.G. Dorner, K.C. Sheehan, R.D. Schreiber, M. Cella, and M. Colonna. 2002. IFN-producing cells respond to CXCR3 ligands in the presence of CXCL12 and secrete inflammatory chemokines upon activation. *J. Immunol.* 169:6079–6083.
18. Pablos, J.L., A. Amara, A. Bouloc, B. Santiago, A. Caruz, M. Galindo, T. Delaunay, J.L. Virelizier, and F. Arenzana-Seisdedos. 1999. Stromal-cell derived factor is expressed by dendritic cells and endothelium in human skin. *Am. J. Pathol.* 155:1577–1586.
19. Nakano, H., M. Yanagita, and M.D. Gunn. 2001. $CD11c^+$ $B220^+$ $Gr\text{-}1^+$ cells in mouse lymph nodes and spleen display characteristics of plasmacytoid dendritic cells. *J. Exp. Med.* 194:1171–1178.
20. Borgland, S.L., G.P. Bowen, N.C. Wong, T.A. Libermann, and D.A. Muruve. 2000. Adenovirus vector-induced expression of the C-X-C chemokine IP-10 is mediated through capsid-dependent activation of NF-kappaB. *J. Virol.* 74:3941–3947.
21. Bussfeld, D., M. Nain, P. Hofmann, D. Gemsa, and H. Sprenger. 2000. Selective induction of the monocyte-attracting chemokines MCP-1 and IP-10 in vesicular stomatitis virus-infected human monocytes. *J. Interferon Cytokine Res.* 20:615–621.
22. Mahalingam, S., G. Chaudhri, C.L. Tan, A. John, P.S. Foster, and G. Karupiah. 2001. Transcription of the interferon gamma (IFN-gamma)-inducible chemokine Mig in IFN-gamma-deficient mice. *J. Biol. Chem.* 9:7568–7574.
23. Reinhart, T.A., B.A. Fallert, M.E. Pfeifer, S. Sanghavi, S. Capuano, III, P. Rajakumar, M. Murphey-Corb, R. Day, C.L. Fuller, and T.M. Schaefer. 2002. Increased expression of the inflammatory chemokine CXC chemokine ligand 9/monokine induced by interferon-gamma in lymphoid tissues of rhesus macaques during simian immunodeficiency virus infection and acquired immunodeficiency syndrome. *Blood.* 99:3119–3128.
24. Jahnsen, F.L., F. Lund-Johansen, J.F. Dunne, L. Farkas, R. Haye, and P. Brandtzaeg. 2000. Experimentally induced recruitment of plasmacytoid (CD123high) dendritic cells in human nasal allergy. *J. Immunol.* 165:4062–4068.
25. Farkas, L., K. Beiske, F. Lund-Johansen, P. Brandtzaeg, and F.L. Jahnsen. 2001. Plasmacytoid dendritic cells (natural interferon-alpha/beta-producing cells) accumulate in cutaneous lupus erythematosus lesions. *Am. J. Pathol.* 159:237–243.
26. Chaperot, L., N. Bendriss, O. Manches, R. Gressin, M. Maynadie, F. Trimoreau, H. Orfeuvre, B. Corront, J. Feuillard, J.J. Sotto, et al. 2001. Identification of a leukemic counterpart of the plasmacytoid dendritic cells. *Blood.* 97:3210–3217.
27. Petrella, T., S. Dalac, M. Maynadie, F. Mugneret, E. Thomine, P. Courville, P. Joly, B. Lenormand, L. Arnould, J. Wechsler, et al. 1999. CD4+ CD56+ cutaneous neoplasms: a distinct hematological entity? Groupe Francais d'Etude des Lymphomes Cutanes (GFELC). *Am. J. Surg. Pathol.* 23:137–146.